Association Between Possible Osteoporosis and Shunt-Dependent Hydrocephalus After Subarachnoid Hemorrhage

Myung-Hoon Han, MD; Yu Deok Won, MD; Min Kyun Na, MD; Choong Hyun Kim, MD, PhD;
Jae Min Kim, MD, PhD; Je Il Ryu, MD, PhD; Hyeong-Joong Yi, MD, PhD; Jin Hwan Cheong, MD, PhD

***Background and Purpose*—**Pathological obstruction in arachnoid granulations after subarachnoid hemorrhage (SAH) can impede cerebrospinal fluid flow outward to the venous sinus and causing hydrocephalus. Because bone and arachnoid granulations share the same collagen type, we evaluated the possible relation between bone mineral density and shunt-dependent hydrocephalus after SAH.

***Methods*—**We measured Hounsfield units of the frontal skull on admission brain computed tomography in patients with SAH. Receiver operating characteristic curve analysis was performed to determine the optimal cutoff Hounsfield unit in skull to predict osteopenia and osteoporosis in a large sample registry. According to the optimal cutoff skull Hounsfield unit values, study patients were then categorized as hypothetical normal, osteopenia, and osteoporosis. Odds ratios were estimated using logistic regression to determine whether the osteoporotic conditions are independent predictive factors for the development of shunt-dependent hydrocephalus after clipping for SAH.

***Results*—**A total of 447 patients (alive ≥14 days) with ruptured aneurysm SAH who underwent surgical clipping were retrospectively enrolled in this study during a 9-year period from 2 hospitals. We found that hypothetical osteoporosis was an independent predictor for shunt-dependent hydrocephalus after aneurysmal clipping for SAH after full adjustment for other predictive factors, including age (odds ratio, 2.08; 95% confidence interval, 1.06–4.08; *P*=0.032).

***Conclusions*—**Our study demonstrates a possible relation between possible osteoporosis and hydrocephalus after SAH. Hounsfield unit measurement on admission brain computed tomography may be helpful for predicting hydrocephalus during the clinical course of SAH in patients with osteoporosis or suspected osteoporosis. **(*Stroke*. 2018;49:1850-1858. DOI: 10.1161/STROKEAHA.118.021063.)**

Key Words: arachnoid ■ bone density ■ hemorrhage ■ hydrocephalus ■ osteoporosis

Hydrocephalus is a common complication after ruptured aneurysm subarachnoid hemorrhage (SAH), and the incidence of shunt-dependent hydrocephalus (SDHC) after SAH has been reported to range from 8.9% to 36.9%.[1] The acute phase of hydrocephalus after SAH shows self-limitation or alleviation after external ventricular drainage insertion in some patients. However, some patients present persistent hydrocephalus ultimately necessitating a ventriculoperitoneal shunt. Therefore, it is important to evaluate the risk factors of hydrocephalus for optimal management while avoiding the increased neurological morbidity and impaired functional outcome associated with chronic hydrocephalus.[2]

Pathological obstruction of arachnoid granulations by blood clots after SAH impedes cerebrospinal fluid (CSF) flow outward to the venous sinus, leading to hydrocephalus.[3] The arachnoid trabeculae are thin, delicate, abundant strands of collagen tissue connecting the space between the arachnoid and pia mater, which is filled with CSF. The primary function of the arachnoid trabeculae is maintaining the stability of the subarachnoid space and CSF flow.[4] In addition, the arachnoid granulations allow the clearance of CSF from the subarachnoid space into the venous system.[5] Both the arachnoid trabeculae and granulations are composed of type 1 collagen,[6] which is also the principal component of the bone matrix protein (90%).[7] Because the bone and arachnoid trabeculae and granulations are composed of the same collagen type, we initiated this study to evaluate the possible association between bone mineral density (BMD) and hydrocephalus after SAH.[6,8,9] We hypothesized that an osteoporotic condition may negatively influence the integrity of the arachnoid trabeculae, as well as bone, and this possible mechanism may be associated with hydrocephalus after SAH. Previous studies

Received February 12, 2018; final revision received May 15, 2018; accepted May 31, 2018.

From the Department of Neurosurgery, Hanyang University Guri Hospital, Korea (M.-H.H., Y.D.W., M.K.N., C.H.K., J.M.K., J.I.R., J.H.C.); and Department of Neurosurgery, Hanyang University Medical Center, Seoul, Korea (H.-J.Y.).

The online-only Data Supplement is available with this article at https://www.ahajournals.org/journal/str/doi/suppl/10.1161/STROKEAHA.118.021063.

Correspondence to Jin Hwan Cheong, MD, PhD, Department of Neurosurgery, Hanyang University Guri Hospital, 153 Gyeongchun-ro, Guri 471–701, Gyonggi-do, Korea. Email cjh2324@hanyang.ac.kr

indicated that Hounsfield unit (HU) values from computed tomographic (CT) scans may be an alternative method for determining regional BMD.[10–13]

We measured HU values in the frontal skull in patients with SAH and examined the relation between BMD and SDHC after SAH based on skull HU values and BMD data from a large sample registry.

Materials and Methods

The data that support the findings of this study are available from the corresponding author on reasonable request.

Study Patients

We retrospectively extracted data for all consecutive primary ruptured aneurysm patients with SAH (>18 years old) from the database of patients with hemorrhagic stroke admitted to the Department of Neurosurgery of Hanyang University Medical Center (Seoul and Guri), Korea, from January 1, 2008, to December 31, 2016. Because of a preference for clipping in patients with SAH at the Guri hospital, we excluded all coiling cases from both hospitals, which may reduce the possible effect of treatment heterogeneity between clipping and coiling on the development of hydrocephalus after SAH. A total of 544 patients was initially identified from the 2 hospitals, and 97 were excluded for the following reasons: (1) death within 2 weeks after aneurysmal clipping (73 patients), (2) postoperative hemorrhagic complications (10 patients), and (3) not possible to measure HU values in cancellous bone because of excessively narrow intercortical space of the frontal skull (14 patients). The remaining 447 patients who underwent aneurysmal clipping for spontaneous SAH were included in the study. All patients had no previous history of SAH, and all surgical clipping procedures were performed within 24 hours of SAH diagnosis in the emergency room.

This study was approved by the institutional review boards of both hospitals. Owing to the retrospective nature of the study, the requirement for informed consent was waived.

Surgery and Management

All operations were performed by 3 faculty neurosurgeons. Surgical techniques and patient management were similar across the 3 neurosurgeons, who trained in the same hospital (Dr Yi in Seoul and Drs Kim and Cheong in Guri). All patients with SAH were treated using a routine SAH treatment protocol, which includes intracranial pressure control with mannitol, anticonvulsant agent, triple-H (hypervolemia/hypertension/hemodilution) therapy, and administration of nimodipine. ventriculoperitoneal shunts were performed when patients had hydrocephalus-related symptoms with the presence of ventricular enlargement and no evidence of blood clots on CT scans during the clinical course of SAH after clipping. We also performed ventriculoperitoneal shunts in patients showing failure of CSF drainage weaning who required chronic external ventricular drainage.

Radiographic and Clinical Variables

We investigated several possible predictive variables for the development of SDHC after SAH. All patients' medical records and radiological findings were reviewed using the electronic medical records and picture archiving and communication system. Radiographic variables, including modified Fisher grade, aneurysm location, accompanying intraventricular hemorrhage, intracerebral hemorrhage, and hydrocephalus on admission, were identified and confirmed by 2 faculty neurosurgeons blinded to the clinical data. The clinical data and operative findings, including sex, age, Hunt-Hess grade, operation type, fenestration of the lamina terminalis, vasospasm, and ventriculoperitoneal shunt, were recorded from medical and operative records. Vasospasm was defined as presenting neurological symptoms with angiographic spasms detected by digital subtraction angiography, CT angiography, or perfusion CT. Hydrocephalus on admission was defined as Evans ratio >0.30 on admission brain CT scan.

Skull HU and BMD Registry Patients

The Skull HU and BMD (SHUB) registry was recently established for various research purposes in our hospital. We retrospectively collected data from patients (>18 years old) having at least ≥1 procedure codes for dual-energy X-ray absorptiometry (DXA; NMF03) and brain CT (RCG01A and B) among all patients who visited or were admitted to Hanyang University Guri hospital from January 1, 2010, to December 31, 2016. Initially, a total of 1825 patients who received at least 1 DXA and brain CT scan for any purpose was identified. When patients underwent multiple DXA scans, we used the lowest T score among the DXA T-score values. In patients who underwent multiple brain CT scans, we selected the brain CT performed closest to the date of the selected DXA scan. We then excluded 361 patients with >3 years between DXA and brain CT to reduce time interval heterogeneity. A previous study reported that osteoporosis would develop in <10% of older women (≥65 years of age) during BMD rescreening intervals of ≈15 years for women with normal bone density or mild osteopenia, 5 years for women with moderate osteopenia, and 1 year for women with advanced osteopenia.[14] According to this finding of relatively slow progression to osteoporosis in older women, we think that the defined time interval (within 3 years) between DXA and brain CT in the registry may be tolerable for the analysis of an association between SHUB. Additionally, 51 patients were excluded who presented no measurable cancellous bone (excessively narrow space between both cortical bones) in the frontal skull. The remaining 1413 patients were included in the registry.

All patients in the SHUB registry underwent BMD (g/cm^2) assessment of the lumbar spine (L1-L4) and femoral neck using the Discovery Wi DXA system (Hologic, Bedford, MA) by licensed technicians. The BMD values were converted into T scores. T-score reference ranges for healthy young Asian female and male subjects were provided by a bone densitometry manufacturer. The lower T score between the lumbar spine and femoral neck was defined as the T score for the registry. Osteoporosis defined as T score ≤−2.5, osteopenia as T score >−2.5 and ≤−1.0, and normal BMD as T score >−1.0, in accordance with the World Health Organization T-score classification.

This study was approved by the institutional review board of our hospital. Because of the retrospective nature of the study, the need for informed consent was waived.

Measurement of Frontal Skull HU

All CT images were obtained with Philips and Siemens CT scanners in the study cohort and Siemens CT scanners in the SHUB registry, with continuous slices, no gap, and 4.0- to 5.0-mm slice thickness. A previous study indicated that variations in HU values across 9 tissue types and 5 CT scanners, including Philips and Siemens, were in the range of 0 to 20 HU.[15] All frontal skull HU measurements in the study and SHUB registry cohorts were conducted by 2 faculty neurosurgeons blinded to patients' clinical data. We used the initial CT images performed in the emergency room in all study patients.

We measured the HU value at each of 4 lines on the frontal bone between the right and left coronal sutures to minimize measurement bias using a picture archiving and communication system that automatically calculates the maximum, minimum, and mean HU values according to the values on the drawn line (linear histogram graph function in the picture archiving and communication system), and we recorded the mean HU value on each line for the present study (Figure 1). It was necessary to establish relatively consistent sites for HU measurement on the frontal bone to reduce variations in HU values depending on regional skull heterogeneity. Therefore, we measured HU values of the frontal skull on axial CT slices at the point where the lateral ventricles disappear. After numerous HU measurement trials, we agreed that the CT level at the disappearance of the lateral ventricle was appropriate for HU measurement because it was convenient and frequently showed relatively thick cancellous bone in

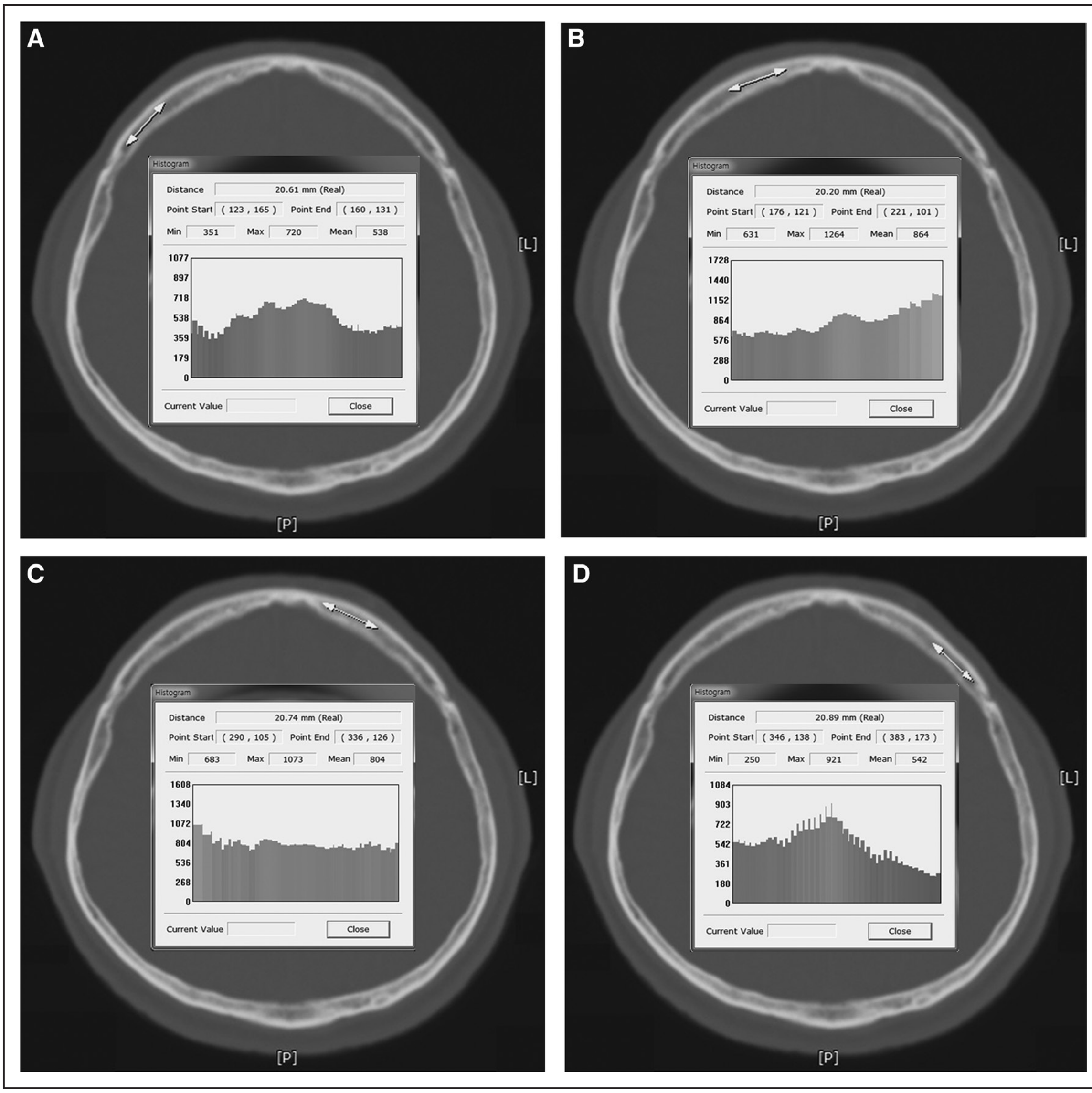

Figure 1. Measurement of Hounsfield unit (HU) values at each of 4 lines on the frontal bone. The picture archiving and communication system automatically calculates the maximum, minimum, and mean HU values according to the values on the drawn line, and the mean HU value on each of the 4 lines was recorded. **A**, Right lateral; (**B**), right medial; (**C**), left medial; (**D**), left lateral.

the frontal skull. When we measured the HU values in the cancellous bone of the frontal skull, all brain CT images were magnified on the bone setting to avoid, including cortical bone, especially in patients with a narrow intercortical space in the frontal bone.

Statistical Methods

The χ^2 test and Student t test were used for discrete and continuous variables, respectively, to identify differences between the non-SDHC and SDHC groups. We used the mean skull HU value (sum of the mean right lateral, right medial, left medial, and left lateral HU values divided by 4) in all analyses.

We also performed linear regression analysis to evaluate associations between T score and mean skull HU value in patients in the SHUB registry.

Receiver operating characteristic (ROC) curve analysis was performed to determine the optimal cutoff skull HU value for predicting osteopenia and osteoporosis in the SHUB registry patients, defined as showing the shortest distance from the upper left corner (where sensitivity=1 and specificity=1). The distance between each point on the ROC curve and the upper left corner was calculated as $\sqrt{(1-\text{sensitivity})^2+(1-\text{specificity})^2}$.[16] We used mean individual skull HU values as the test variable and the individual BMD classification as the state variable (dependent variable) in the ROC curve analysis. To determine the cutoff skull HU value for predicting osteopenia, we set the normal BMD (T score >−1.0) as coding 0 and the T score ≤−1.0 as coding 1 and input the state variable. Similarly, we set the T score >−2.5 as coding 0 and the osteoporosis (T score ≤−2.5) as coding 1 and input the state variable in the osteoporosis model. Visualization of the ROC curve was performed using the plot.roc function of the R software.

Odds ratios (ORs) with 95% confidence intervals (CIs) were estimated using univariate and multivariate logistic regressions to determine whether the osteoporotic conditions are the independent predictive factors for the development of SDHC after clipping for SAH. Sex, age, Hunt-Hess grade, modified Fisher grade, aneurysm location, intraventricular hemorrhage, hypothetical BMD classification, intracerebral hemorrhage, operation type, fenestration of the lamina terminalis, vasospasm, and hydrocephalus on admission were entered into the multivariate model. We chose covariates in addition to sex, age, and hypothetical BMD classification in the multivariate analysis based on the following criteria: (1) generally accepted possible predictive factors for SDHC after SAH[1] and (2) 2 surgical factors (operation type and fenestration of the lamina terminalis), which can be reasonably considered as predictive factors for SDHC.

All statistical analyses were performed using R software, version 3.3.3 (https://www.r-project.org/).

Results

Determination of the Optimal Skull HU Values to Predict Osteopenia and Osteoporosis

We observed a significant positive correlation between the T score and mean frontal skull HU value among patients in the SHUB registry (Figure 2A). The result of the linear regression analysis demonstrated an ≈107 increase of mean skull HU per 1 T-score increase (B=107.24; $P<0.001$). The optimal cutoff values of the mean skull HU for prediction of osteopenia and osteoporosis in the patients from the SHUB registry were 719.875 (area under the curve, 0.811; sensitivity, 75.2%; specificity, 74.3%; $P<0.001$) and 601.375 (area under the curve, 0.776; sensitivity, 72.3%; specificity, 70.5%; $P<0.001$), respectively (Figure 2B). According to the results, the study patients were then categorized as hypothetical normal (above the cutoff HU value of osteopenia [>719.875]), osteopenia (between the cutoff HU values for osteopenia and osteoporosis [>601.375 and ≤719.875]), and osteoporosis (below the cutoff HU value for osteoporosis [≤601.375]). The association between each of the 4 HU values of the frontal bone and T-score is in the online-only Data Supplement. The slope of the linear regression line was similar between the right and left medial (B=113.774 and B=114.389, respectively) and between the right and left lateral (B=100.268 and B=100.550, respectively).

Characteristics of the Study Patients

Four hundred forty-seven patients (>18 years of age) alive ≥14 days with primary spontaneous ruptured aneurysm SAH who

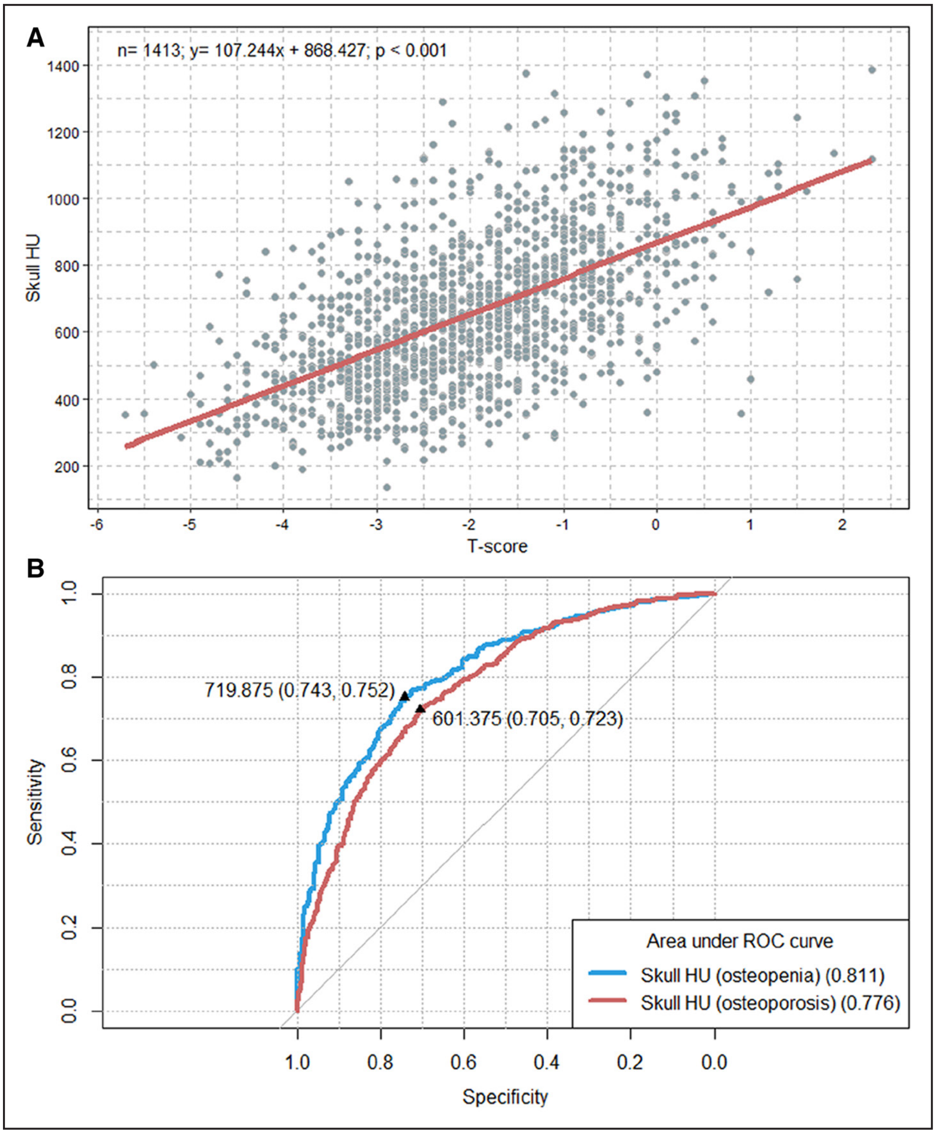

Figure 2. Scatter plot with the linear regression line and receiver operating characteristic (ROC) curve. **A**, Linear regression line showing the association between T score and mean skull Hounsfield unit (HU) in patients from the Skull HU and Bone Mineral Density (SHUB) registry; (**B**) ROC curve to identify the optimal cutoff skull HU values for prediction of osteopenia and osteoporosis from the SHUB registry.

Table 1. Characteristics of Patients With Primary Spontaneous SAH Who Underwent Surgical Clipping Classified According to SDHC in the Study Cohort

Characteristics	SDHC (−)	SDHC (+)	Total	*P* Value
n	367	80	447	
Sex, women, n (%)	231 (62.9)	57 (71.3)	288 (64.4)	0.197
Age, y; mean±SD	53.5±11.6	60.0±11.1	54.7±11.7	<0.001
Time interval between SAH and shunting, d; median (IQR)	NA	52.5 (32.5–74.0)	NA	
Hunt-Hess grade, n (%)				<0.001
1	28 (7.6)	1 (1.3)	29 (6.5)	
2	186 (50.7)	25 (31.3)	211 (47.2)	
3	106 (28.9)	26 (32.5)	132 (29.5)	
4	44 (12.0)	26 (32.5)	70 (15.7)	
5	3 (0.8)	2 (2.5)	5 (1.1)	
Modified Fisher grade, n (%)				0.001
1	68 (18.5)	10 (12.5)	78 (17.4)	
2	33 (9.0)	10 (12.5)	43 (9.6)	
3	113 (30.8)	10 (12.5)	123 (27.5)	
4	153 (41.7)	50 (62.5)	203 (45.4)	
Location, n (%)				0.233
ACA	123 (33.5)	34 (42.5)	157 (35.1)	
MCA	122 (33.2)	18 (22.5)	140 (31.3)	
ICA	19 (5.2)	5 (6.3)	24 (5.4)	
PCOM	97 (26.4)	20 (25.0)	117 (26.2)	
VBA	6 (1.6)	3 (3.8)	9 (2.0)	
IVH, n (%)	186 (50.7)	60 (75.0)	246 (55.0)	<0.001
Classification of mean skull HU, n (%)				0.002
Hypothetical normal (>719.9)	236 (64.3)	37 (46.3)	273 (61.1)	
Hypothetical osteopenia (>601.4 and ≤719.9)	69 (18.8)	16 (20.0)	85 (19.0)	
Hypothetical osteoporosis (≤601.4)	62 (16.9)	27 (33.8)	89 (19.9)	
ICH, n (%)	99 (27.0)	23 (28.8)	122 (27.3)	0.782
Craniectomy, n (%)	34 (9.3)	20 (25.0)	54 (12.1)	<0.001
Fenestration of the lamina terminalis, n (%)	111 (30.2)	26 (32.5)	137 (30.6)	0.690
Vasospasm, n (%)	116 (31.6)	24 (30.0)	140 (31.3)	0.894
Evans ratio on admission, mean±SD	0.25±0.04	0.27±0.04	0.26±0.04	0.001
Hydrocephalus on admission, n (%)	32 (8.7)	18 (22.5)	50 (11.2)	0.001

ACA indicates anterior cerebral artery; HU, Hounsfield unit; ICA, internal carotid artery; ICH, intracerebral hemorrhage; IQR, interquartile range; IVH, intraventricular hemorrhage; MCA, middle cerebral artery; NA, not available; PCOM, posterior communicating artery; SAH, subarachnoid hemorrhage; SDHC, shunt-dependent hydrocephalus; and VBA, vertebrobasilar artery.

underwent surgical clipping were enrolled in this study during a 9-year period from 2 university hospitals. The mean patient age was 54.7 years, and 64.4% of patients were women. A total of 80 patients was treated with ventriculoperitoneal shunts for hydrocephalus after SAH. Non-SDHC and SDHC patients demonstrated significant differences in age, Hunt-Hess grade, modified Fisher grade, intraventricular hemorrhage, classification of mean skull HU, craniectomy, and hydrocephalus on admission. Further details of the study patients are presented in Table 1.

Descriptive Statistics of SHUB

Table 2 shows descriptive statistics for sex, age, and skull HU in both registries, with additional BMD information for the SHUB registry. The SHUB registry patients demonstrated a greater female predominance and older age distribution compared with those in the study cohort. The median of overall mean skull HU was 786.8 in the study cohort and 626.8 in the SHUB registry. The median time interval between brain CT and BMD was 188 days, and 537 (38.0%) patients demonstrated osteoporosis, with mean T score of −2.03, in the SHUB registry.

Table 2. Descriptive Statistics of the Study and SHUB Registry Cohorts

Variables	Study Cohort	SHUB Registry
n	447	1413
Sex		
Women, n (%)	288 (64.4)	1187 (84.0)
Age, y; median (IQR)	53 (47–62)	68 (58–75)
Overall mean skull HU value, median (IQR)	786.8 (631.8–1007.3)	626.8 (483.1–795.5)
Overall mean skull HU value, mean±SD	837.1±287.3	650.7±225.8
Mean HU value at each of 4 sites in the frontal skull, mean±SD		
Right lateral	762.9±273.4	602.5±216.4
Right medial	915.0±322.9	690.7±250.7
Left medial	902.2±321.5	690.9±253.6
Left lateral	768.1±280.1	618.9±221.4
Average, medial	908.6±317.4	690.8±247.8
Average, lateral	765.5±271.3	610.7±214.0
Time interval between brain CT and BMD, d; median (IQR)	NA	188 (11–544)
T score, mean±SD	NA	−2.03±1.23
Lumbar spine	NA	−1.71±1.45
Femur neck	NA	−1.38±1.23
BMD categories, n (%)		
Normal (T score >−1.0)	NA	269 (19.0)
Osteopenia (T score >−2.5 and ≤1.0)	NA	607 (43.0)
Osteoporosis (T score ≤−2.5)	NA	537 (38.0)

BMD indicates bone mineral density; CT, computed tomography; HU, Hounsfield unit; IQR, interquartile range; NA, not available; and SHUB, skull Hounsfield unit and bone mineral density.

Independent Predictive Factors for SDHC Occurrence After SAH

The results of univariate logistic regression analysis are shown in Table 3. Multivariate logistic analysis identified the hypothetical osteoporosis (OR, 2.08; 95% CI, 1.06–4.08; P=0.032) as an independent predictor of SDHC after aneurysmal clipping for SAH (Figure 3). However, hypothetical osteopenia was not statistically significant (OR, 1.13; 95% CI, 0.55–2.33; P=0.734). The additional independent predictors of SDHC after SAH were older age, higher Hunt-Hess grade, accompanying intraventricular hemorrhage, and hydrocephalus on admission.

Although we adjusted age as a continuous covariate in the multivariate analysis, it is generally accepted that a higher incidence of both SDHC after SAH and osteoporosis is seen in old age. Therefore, we further investigated the incidence of SDHC after SAH based on the age group according to hypothetical osteoporosis in the study cohort (Table I in the online-only Data Supplement). We found a 2-fold higher SDHC occurrence with statistical significance in the hypothetical osteoporosis group than in the nonhypothetical osteoporosis group among the older patients (≥65 years of age; 43.5% versus 20.0%, respectively; P=0.012). In addition, multivariate analysis showed a significantly increased risk of SDHC in the hypothetical osteoporosis group in the old age group (≥65 years of age; OR, 3.87; 95% CI, 1.34–11.18; P=0.013; Table II in the online-only Data Supplement).

We performed additional multivariate logistic analysis after exclusion for patients with hydrocephalus on admission because initial hydrocephalus after SAH may modify the exposure outcome relationship (Table III in the online-only Data Supplement). The patients with hypothetical osteoporosis after exclusion for patients with initial hydrocephalus showed more significant association with SDHC compared with the study cohort (OR, 2.97; 95% CI, 1.41–6.22; P=0.004). In addition, we found that hypothetical osteoporosis showed the most significant relationship with SDHC among all predictive factors, including age and Hunt-Hess grade, after exclusion for patients with hydrocephalus on admission.

Discussion

We found that the hypothetical osteoporosis group (mean skull HU, ≤601.4) had an ≈2.1-fold increased risk of SDHC compared with the hypothetical normal group (mean skull HU, >719.9) after aneurysmal clipping for SAH after adjusting for other predictive factors, including age. A significant linear correlation was observed between T score and skull HU values in the SHUB registry. In addition, the cutoff skull HU values determined by ROC curve analysis with a large sample size showed >70% specificity and sensitivity of osteopenia and osteoporosis. Therefore, we think that HU measurement in the frontal cancellous bone may be predictive of osteoporotic conditions.

The HU value in a specific anatomic area on CT is an accurate absolute value with validity and reproducibility in all appropriately calibrated CT scanners, with variation in the range of 0 to 20 HU.[15,17] BMD is also reported in absolute values, including Z score (comparison with age-, race-, and sex-matched reference range) and T score (comparison with mean bone mass of healthy young adults).[18] We think that the association between the absolute values of HU and T score, may not be affected by different characteristics of patients between the study cohort and SHUB registry. This is because patient characteristics may affect bone quality, but HU values of bone and BMD are methods to evaluate the bone density that yield absolute values. Therefore, the simple relationship between HU values and BMD may not be affected by patient characteristics and should be linear even if the cohort is highly heterogenous.

Because osteoporosis is a systemic disease that affects systemic bone mass and microarchitecture throughout the body, we hypothesized that osteoporotic conditions may influence structures of the cancellous bone in the skull.[19] Similar to our study, a previous study proposed opportunistic screening for osteoporosis in heterogeneous patients using HU values of the lumbar spine from abdominal CT images.[13] Other

Table 3. Univariate Logistic Regression Analysis of Shunt-Dependent Hydrocephalus After Aneurysmal Clipping for Subarachnoid Hemorrhage Based on Predictive Factors in the Study Patients

Variable	Univariate Logistic Regression Analysis	
	OR (95% CI)	*P* Value
Sex		
Men	Reference	
Women	1.46 (0.86–2.48)	0.161
Age, y; (per 1-y increase)	1.05 (1.03–1.07)	<0.001
Hunt-Hess grade		
1–3	Reference	
4 and 5	3.67 (2.11–6.37)	<0.001
Modified Fisher grade		
1 and 2	Reference	
3 and 4	1.14 (0.65–1.99)	0.646
Aneurysm location		
Anterior circulation	Reference	
Posterior circulation	1.03 (0.61–1.77)	0.902
IVH		
No	Reference	
Yes	2.92 (1.69–5.04)	<0.001
Classification of mean skull HU		
Hypothetical normal	Reference	
Hypothetical osteopenia	1.48 (0.78–2.82)	0.234
Hypothetical osteoporosis	2.78 (1.57–4.91)	<0.001
ICH		
No	Reference	
Present	1.09 (0.64–1.87)	0.747
Operation type		
Craniotomy	Reference	
Craniectomy	3.27 (1.76–6.05)	<0.001
Fenestration of the lamina terminalis		
No	Reference	
Yes	1.11 (0.66–1.86)	0.692
Vasospasm		
No	Reference	
Yes	0.93 (0.55–1.57)	0.779
Hydrocephalus on admission		
No	Reference	
Yes	3.04 (1.61–5.75)	0.001

CI indicates confidence interval; HU, Hounsfield unit; ICH, intracerebral hemorrhage; IVH, intraventricular hemorrhage; and OR, odds ratio.

previous studies also demonstrated that regional cancellous bone HU values from clinical CT scans are strongly correlated with T score and may be useful in detecting osteopenia and osteoporosis.[10–12]

To the best of our knowledge, this study is the first to suggest a possible relation between possible osteoporosis and SDHC after SAH.

Osteoporosis is a common disease with a strong genetic component, and type 1 collagen is the major protein of bone encoded by the *COL1A1* and *COL1A2* genes.[20] The study described that G/T heterozygotes at the polymorphic Sp1 site in a regulatory region of COL1A1 demonstrated significantly lower BMD than G/G homozygotes. Furthermore, osteogenesis imperfecta caused by heterozygous mutations in the type 1 procollagen genes (*COL1A1*/*COL1A2*) is associated with communicating hydrocephalus.[21,22] Therefore, we hypothesized that an osteoporotic condition with a strong genetic component (ie, type 1 collagen genes) leading to systemic disease may negatively influence the integrity of arachnoid trabeculae and granulation, which are also composed of type 1 collagen. Based on this hypothesis, we think that the after hypothetical mechanism may be a possible explanation for the association between possible osteoporosis and hydrocephalus after SAH in the study. After SAH occurrence, the integrity of arachnoid granulations and trabeculae in the subarachnoid space may be relatively maintained among those with a dense and strong type 1 collagen tissue compared to weak one. The relatively maintained integrity of arachnoid trabeculae and granulations may lead to CSF outflow to the venous system more efficiently with maintaining stability of the subarachnoid space and CSF flow through it compared to patients with more damaged or weaker arachnoid trabeculae and granulations.

Our study has several limitations. First, the actual T-score was not available for patients from the study cohort. Initially, we tried to investigate actual T-scores in patients with SAH. However, few patients had actual T-scores from incidental DXA scans, and the time intervals between DXA and brain CT for SAH were highly heterogeneous because patients with SAH typically do not have a necessity to undergo DXA scans. However, we think that our study is valuable because we evaluated the possible link between possible osteoporosis and hydrocephalus after SAH based on the observed close correlation between skull HU and T score from large sample size. Second, HU measurement errors may have occurred, especially in patients with a narrow intercortical space in the frontal bone. However, all brain CT images were magnified for HU measurement, and we initially excluded patients with an intercortical space in frontal skull that was too narrow for measurement. In addition, to reduce measurement errors, we calculated mean HU values in 4 areas of the frontal skull and averaged them. Third, to the best of our knowledge, there are no histological studies showing a direct link between osteoporosis and arachnoid trabeculae. Therefore, our proposed mechanisms are hypothetical. We think it will be valuable to investigate the association between osteoporosis and arachnoid trabeculae in the future. Fourth, there was a potential difference in the cutoff value for osteopenia and osteoporosis between men and women. Therefore, there was potential for misclassifying men because the cutoff values were derived from mostly women in the SHUB registry. Fifth, time intervals between SAH and shunting in our study seem to be longer than those in previous studies.[1] However, shunting time after SAH is also heterogeneous among previous studies and likely depends on various

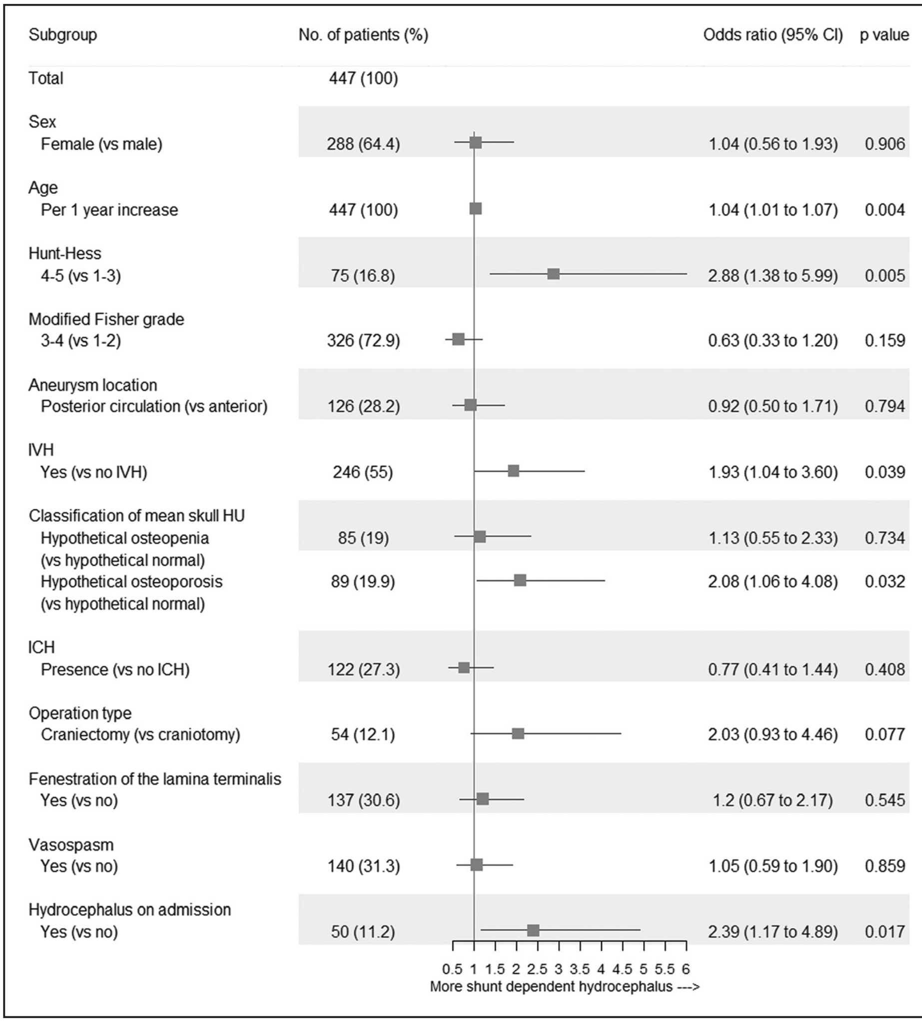

Figure 3. Forest plot of estimates from the multivariate logistic regression analysis for predicting shunt-dependent hydrocephalus occurrence according to the potential predictive factors (adjusted for sex, age [continuous variable], Hunt-Hess grade, modified Fisher grade, aneurysm location, intraventricular hemorrhage (IVH), skull Hounsfield unit (HU), intracerebral hemorrhage (ICH), operation type, fenestration of the lamina terminalis, and vasospasm) in the study patients. CI indicates confidence interval.

patient conditions, hospital protocol, and physician preferences. A recent study found that delayed ventriculoperitoneal shunting (>40 days) occurred frequently, and early shunting was significantly associated with coil embolization.[23] Last, this study may generate a hypothesis that will need to be tested in a prospective study using a priori definitions for shunt insertion. Nevertheless, we expect that this study will expand our understanding of hydrocephalus after SAH.

In conclusion, our study showed a close relationship between frontal SHUB and a possible relation between possible osteoporosis and hydrocephalus after SAH. We think that our findings have value for predicting osteoporotic conditions using a convenient method for measuring HU of the frontal skull on brain CT. Additionally, we think these findings may be helpful for predicting hydrocephalus during the clinical course of SAH in patients with osteoporosis or suspected osteoporosis based on HU measurement on admission brain CT.

Sources of Funding

This work was supported by the research fund of Hanyang University (HY- 201600000002777).

Disclosures

None.

References

1. Xie Z, Hu X, Zan X, Lin S, Li H, You C. Predictors of shunt-dependent hydrocephalus after aneurysmal subarachnoid hemorrhage? A systematic review and meta-analysis. *World Neurosurg*. 2017;106:844–860.e6. doi: 10.1016/j.wneu.2017.06.119.
2. Adams H, Ban VS, Leinonen V, Aoun SG, Huttunen J, Saavalainen T, et al. Risk of shunting after aneurysmal subarachnoid hemorrhage: a collaborative study and initiation of a consortium. *Stroke*. 2016;47:2488–2496. doi: 10.1161/STROKEAHA.116.013739.
3. Chen S, Luo J, Reis C, Manaenko A, Zhang J. Hydrocephalus after subarachnoid hemorrhage: pathophysiology, diagnosis, and treatment. *Biomed Res Int*. 2017;2017:8584753. doi: 10.1155/2017/8584753.
4. Mortazavi MM, Quadri SA, Khan MA, Gustin A, Suriya SS, Hassanzadeh T, et al. Subarachnoid trabeculae: a comprehensive review of their embryology, histology, morphology, and surgical significance. *World Neurosurg*. 2018;111:279–290. doi: 10.1016/j.wneu.2017.12.041.
5. Kapoor KG, Katz SE, Grzybowski DM, Lubow M. Cerebrospinal fluid outflow: an evolving perspective. *Brain Res Bull*. 2008;77:327–334. doi: 10.1016/j.brainresbull.2008.08.009.
6. Saboori P, Sadegh A. Histology and morphology of the brain subarachnoid trabeculae. *Anat Res Int*. 2015;2015:279814. doi: 10.1155/2015/279814.

7. Clines GA. Prospects for osteoprogenitor stem cells in fracture repair and osteoporosis. *Curr Opin Organ Transplant*. 2010;15:73–78. doi: 10.1097/MOT.0b013e328333d52c.
8. Abraham K, Laura T. *Histology and Cell Biology: An Introduction to Pathology*. 4th ed. Philadelphia, PA: Saunders; 2015.
9. van der Rest M, Garrone R. Collagen family of proteins. *FASEB J*. 1991;5:2814–2823.
10. Johnson CC, Gausden EB, Weiland AJ, Lane JM, Schreiber JJ. Using Hounsfield units to assess osteoporotic status on wrist computed tomography scans: comparison with dual energy X-ray absorptiometry. *J Hand Surg Am*. 2016;41:767–774. doi: 10.1016/j.jhsa.2016.04.016.
11. Schreiber JJ, Anderson PA, Rosas HG, Buchholz AL, Au AG. Hounsfield units for assessing bone mineral density and strength: a tool for osteoporosis management. *J Bone Joint Surg Am*. 2011;93:1057–1063. doi: 10.2106/JBJS.J.00160.
12. Choi MK, Kim SM, Lim JK. Diagnostic efficacy of Hounsfield units in spine CT for the assessment of real bone mineral density of degenerative spine: correlation study between T-scores determined by DEXA scan and Hounsfield units from CT. *Acta Neurochir (Wien)*. 2016;158:1421–1427. doi: 10.1007/s00701-016-2821-5.
13. Pickhardt PJ, Pooler BD, Lauder T, del Rio AM, Bruce RJ, Binkley N. Opportunistic screening for osteoporosis using abdominal computed tomography scans obtained for other indications. *Ann Intern Med*. 2013;158:588–595. doi: 10.7326/0003-4819-158-8-201304160-00003.
14. Gourlay ML, Fine JP, Preisser JS, May RC, Li C, Lui LY, et al; Study of Osteoporotic Fractures Research Group. Bone-density testing interval and transition to osteoporosis in older women. *N Engl J Med*. 2012;366:225–233. doi: 10.1056/NEJMoa1107142.
15. Birnbaum BA, Hindman N, Lee J, Babb JS. Multi-detector row CT attenuation measurements: assessment of intra- and interscanner variability with an anthropomorphic body CT phantom. *Radiology*. 2007;242:109–119. doi: 10.1148/radiol.2421052066.
16. Nguyen TT, Adair LS, He K, Popkin BM. Optimal cutoff values for overweight: using body mass index to predict incidence of hypertension in 18- to 65-year-old Chinese adults. *J Nutr*. 2008;138:1377–1382. doi: 10.1093/jn/138.7.1377.
17. Timothy G. *The Mathematics of Medical Imaging: A Beginner's Guide*. 2nd ed. New York: Springer; 2015.
18. Klippel JH, Stone JH, Crofford L Eslie J, White PH. *Primer on the Rheumatic Diseases*. 13th ed. New York: Springer Science & Business Media; 2008.
19. Brandi ML. Microarchitecture, the key to bone quality. *Rheumatology (Oxford)*. 2009;48 suppl 4:iv3–iv8. doi: 10.1093/rheumatology/kep273.
20. Grant SF, Reid DM, Blake G, Herd R, Fogelman I, Ralston SH. Reduced bone density and osteoporosis associated with a polymorphic Sp1 binding site in the collagen type I alpha 1 gene. *Nat Genet*. 1996;14:203–205. doi: 10.1038/ng1096-203.
21. Rolvien T, Kornak U, Stürznickel J, Schinke T, Amling M, Mundlos S, et al. A novel COL1A2 C-propeptide cleavage site mutation causing high bone mass osteogenesis imperfecta with a regional distribution pattern. *Osteoporos Int*. 2018;29:243–246. doi: 10.1007/s00198-017-4224-8.
22. Charnas LR, Marini JC. Communicating hydrocephalus, basilar invagination, and other neurologic features in osteogenesis imperfecta. *Neurology*. 1993;43:2603–2608.
23. Shigematsu H, Sorimachi T, Osada T, Aoki R, Srivatanakul K, Oda S, et al. Predictors of early vs. late permanent shunt insertion after aneurysmal subarachnoid hemorrhage. *Neurol Res*. 2016;38:600–605. doi: 10.1080/01616412.2016.1199184.